

STANISŁAW STRYCZEK*, RAFAŁ WIŚNIOWSKI*

RHEOLOGICAL MODELS OF SALINE SEALING SLURRIES WITH FLY ASHES CONTENT

MODELE REOLOGICZNE SOLANKOWYCH ZACZYNÓW USZCZELNIAJĄCYCH Z DODATKIEM POPIOŁÓW LOTNYCH

The criteria which should be taken into consideration when selecting sealing slurries based on fly ashes for injection operations in a saline rock mass are presented in this paper. Cement-ash cements are analysed and tabulated qualitatively. The results of laboratory analyses aiming at establishing the rheological parameters of the sealing slurries are also included.

The principles for the selection of a rheological model of the slurry are discussed and the relevant relationships influencing this the selection are given.

Based on the results, the physico-chemical effects taking place in the saline sealing slurries were analysed. Later in the paper the influence of these processes on the rheological properties is explained.

Additionally, principles for the calculation of resistivity to flow of slurries are put forward, accounting for the selection of an optimum rheological model for each analysed recipe. The results and an exemplary simulation are highlighted in the conclusion.

Key words: rheology, saline sealing slurries, flow resistivity, rheological models

W artykule przedstawiono kryteria, jakie powinny być rozważane przy doborze solankowych zaczynów uszczelniających sporządzanych na bazie popiołów lotnych do prac inieckijnych w górotworze solnym. Podano charakterystykę spoiw cementowo-popiołowych oraz przedstawiono wyniki badań laboratoryjnych, mających za cel określenie wielkości parametrów reologicznych sporządzanych zaczynów uszczelniających.

Następnie opisano zasady doboru modelu reologicznego zaczynu oraz podano zależności umożliwiające wyznaczanie parametrów reologicznych płynów uszczelniających.

Analizując wyniki badań podano interpretację zjawisk fizykochemicznych zachodzących w sporządzonych solankowych zaczynach uszczelniających oraz wyjaśniono wpływ zachodzących procesów na otrzymywane właściwości reologiczne płynów.

* ZAKŁAD WIERTNICTWA I GEOINŻYNIERII WZNIG AGH, 30-059 KRAKÓW, AL. MICKIEWICZA 30; stryczek@uci.agh.edu.pl,
wisniows@uci.agh.edu.pl

W dalszej części pracy przedstawiono zasady obliczania oporów przepływu zaczynów, uwzględniające dobór optymalnego modelu reologicznego dla każdej rozważanej receptury. Wyniki analiz i przykładowych symulacji sprecyzowano we wnioskach.

Slowa kluczowe: reologia, solankowe zaczyny uszczelniające, opory przepływu, modele reologiczne

1. Introduction

In the course of exploitation activities carried out in salt mines voids are created, constituting a danger for miners and to objects on the surface. The displacement of soil and rocks may damage installations and surface structures, change hydro-geological conditions, and consequently degrade the natural environment. Hence the need to fill the underground voids and neutralise the potential effects of abandoned workings in existing or decommissioned salt mines. The most frequent method used in such a case is filling with liquid substances, which after solidification form a solid body, a sealing monolith.

Backfilling, i.e. filling the underground voids, sealing, reinforcing and isolating a specific rock mass is made with the use of saline sealing slurries. However, if they are to be injected to the rock mass, they have to meet certain requirements.

Firstly, they should be compatible with the immediate environment. The chemical composition of the brine should be compatible with the rock mass as far as its chemical compatibility and solubility are concerned. The liquid to be used should be a fully saturated brine at a temperature corresponding to the ambient temperature of the rock mass.

Secondly, the injectability criterion has to be defined through the proper selection of the rheological model and rheological parameters of the sealing slurry. With well defined rheological parameters it is possible to calculate the flow resistivity of the slurry in the introduction system from the injection devices to the place of destination. Knowing the hydraulic frictional pressure loss techniques and technology for filling the voids may be selected on a rational basis.

A third condition is to maintain the strength of the hardened sealing slurries, formed by the physico-chemical processes. The recipes of the slurries should be so selected as to provide a solidified mass with good mechanical properties. These should be the same or similar to those of the natural rock mass. Subsidence and deformations in the rock mass are less frequent in a stable and conformable soil and rock mass.

One of the basic criteria for recipe selection is based on economic and environmental issues. To limit the material costs, it is suggested that saline sealing slurries might be admixed with a cheap waste material, i.e. fly ash. The use of waste material and discharge brines may considerably reduce the cost of deposition and limit the environmental impact.

2. Cement-ash cements

In accordance with the Polish Standard PN-B-19701 "Common use cement", there have been selected, among others, ash cements containing silica fly ash (V), a product of coal combustion.

The silica fly ash (V) can be used as an element of:

- main Portland ash cement CEM II and *puzzolan* cement CEM IV
- secondary Portland cement CEM I (to 5% by wt.)

In accordance with the Polish Standard No PN-B-19701, amended according to the requirements of the European Standard ENV 197-1, the following cements have been categorised:

- Portland ash cements CEM II/A-V and CEM II/B-V types, containing respectively 20 and 30% by wt. of silica fly ash,
- *puzzolan* cement CEM IV/A and CEM IV/B types, which may respectively contain up to 35 and 55% by wt. of silica fly ash.

Silica fly ashes have big specific surface from 2000 to 5000 cm²/g, inner porosity 0.6 to 0.7 cm³/g, density 1700 to 2500 kg/m³, bulk weight 600 to 900 kG/m³.

Silica fly ash is chemically active. Its *puzzolan* properties are due to the active silica content. They are manifested in the reactivity with calcium hydroxide in an aqueous environment and the concurrent formation of bonding compounds, mainly CSH phases. Simultaneously, in the liquid phase reactions of calcium and aluminium ions can be observed, in the course of which hydrated calcium aluminates are formed. Finally, in the course of the physico-chemical processes, the easily soluble Ca(OH)₂ content is reduced, and the proportion of desired hydraulic constituents increases. This positively influences the sealing properties of the cement matrix and the properties responsible for the durability of the hardened cement slurry.

Portland cements with fly ash admixtures have recently been used increasingly widely in various engineering applications. They are selected for their advantageous properties, which have been demonstrated in practice.

3. Laboratory tests

The aim of the laboratory tests was to evaluate the technological properties of sealing slurries based on silica fly ashes and Portland cement in the context of sealing operations in a saline rock mass. The recipes of the saline sealing slurries, and their properties with regard to the specific rheological parameters and objectives of the injection project were analysed.

The tests were made on the basis of the following standards:

- Polish Standard PN-85/G02320. Drilling. Cements and slurries for cementing operations in drilling wells,
- API Specification for Materials and Testing for Well Cements. SPEC 10. Fifth Edition 1990.

As a result of the tests the influence of the following elements was established:

- fully saturated brine,
 - silica fly ash concentration (by weight in relation to dry Portland cement)
- on the type of rheological model, and consequently, on rheological parameters for each analysed model.

When making the saline sealing slurries, the following components were used:

- Portland cement CEM I 32.5 R produced by the Cement Company "Górażdże",
- fly ash from the "Kraków S.A." Power-and-Heat Station,
- fully saturated natural brine.

In Table 1 the results of a chemical analysis of natural brine used for the sealing slurry with the water-to-cement ratio equal to 0.6 are shown. The selection of such a value of the water-to-cement ratio is dictated by practice. The resultant fresh and hardened slurries exhibit optimum technological parameters.

TABLE 1

Results of chemical analysis of brine (Stryczek, Gonet 2001)

TABLICA 1

Wyniki analizy chemicznej solanki (Stryczek, Gonet 2001)

Measurement	pH	NaCl [g/l]	Ca ²⁺ [g/l]	Mg ²⁺ [g/l]	Na ⁺ [g/l]	K ⁺ [g/l]	SO ₄ ²⁻ [g/l]
Brine for the sealing slurry	7	300	1.10	0.20	110	2	7.5

The chemical composition of the inorganic binder CEM I 32.5 R by the Cement Company "Górażdże" is shown in Table 2.

TABLE 2

Chemical composition of Portland cement CEM I 32.5 R (Orzeczenie o jakości cementu 2000)

TABLICA 2

Skład chemiczny cementu portlandzkiego CEM I 32.5R (Orzeczenie o jakości cementu 2000)

Chemical composition	SiO ₂	Al ₂ O ₃	Fe ₂ O ₃	CaO	MgO	SO ₃	Specific surface after Blaine [cm ² /g]
%	19.88	4.94	2.64	63.33	1.06	3,03	3385

The chemical composition of ash from the Power-and Heat Station "Kraków S.A." is shown in Table 3.

TABLE 3

Chemical composition of ash (Praca zbiorowa 2000)

TABLICA 3

Skład chemiczny popiołu (Praca zbiorowa 2000)

Measured oxide	Content after burning	Content calculated for the initial state
	[% wt.]	
SiO ₂	50.28	44.55
Al ₂ O ₃	31.98	28.30
Fe ₂ O ₃	6.50	5.75
CaO	3.40	3.00
MgO	2.20	1.95
Na ₂ O	0.85	0.75
K ₂ O	1.36	1.20
SO ₃	0.81	0.72
TiO ₂	0.79	0.70
P ₂ O ₅	0.47	0.42
BaO	0.56	0.50
SrO	<0.01	<0.01
H ₂ O	—	5.65
Burining losses	—	6.42
Total	99.20	99.91
Ash content	93.58	—

Hydraulic binders (Portland cement, fly ash) to be used for sealing slurries were so comminuted that the residues on sieve were less than 2% for a grid of 0.20 mm, and less than 20% for a grid of 0.08 mm (Polish Standard PN-85/G02320. Drilling. Cements and slurries for cementing operations in drilling wells). The temperature of the hydraulic binders and the liquid was 20°C ($\pm 2^\circ\text{C}$) [293K]. Fully saturated natural brine was used (density $\rho = 1200 \text{ kg/m}^3$.)

The measured volume of brine was poured into a plastic cup and a high-speed mixer (1200 rpm) was started. The prepared portions of Portland cement and fly ash were added over the next 15 to 30 seconds, in accordance with the recipe. The total mixing time was 5 minutes.

For test purposes, eight recipes of saline sealing slurries were prepared. The water-to-cement ratio was 0.6, but the concentrations of the solids differed (Table 4). The listed recipes of saline sealing slurries are only a representative selection of the total spectrum of recipes analysed.

TABLE 4

Components of saline sealing slurries

TABLICA 4

Składniki receptury solankowych zaczynów uszczelniających

No.	Measur- ement of slurry	Solids content in the slurry [%]		Water- to-binder ratio w/s	Components necessary for making 1 m ³ of saline sealing slurry			Calculated density of sealing slurry [kg/m ³]
		Portland cement “Górażdze” CEM I 32,5 R	Fly ash (Power-and- -Heat Station “Kraków S.A.”)		Portland cement “Górażdze” CEM I 32,5 R [kg]	Fly ash Power-and- -Heat Station “Kraków S.A.” [kg]	Fully saturated brine [m ³]	
1	BC-1	—	100	0.6	0.0	947.4	0.474	1 516
2	BC-2	10	90	0.6	96.8	871.0	0.484	1 548
3	BC-3	20	70	0.6	197.8	791.2	0.495	1 582
4	BC-4	30	50	0.6	303.4	707.9	0.506	1 618
5	BC-5	50	30	0.6	529.4	529.5	0.529	1 694
6	BC-6	70	20	0.6	777.8	333.3	0.556	1 778
7	BC-7	90	10	0.6	1 100.0	116.9	0.584	1 870
8	BC-8	100	—	0.6	1 200.0	0.0	0.600	1 920

The tests designed to determine the rheological parameters of fresh saline sealing slurries were made with the use of a rotary viscosity meter Chan 35 API Viscometer type. The torsion of the spring Φ_i was measured for twelve different rotation speeds n_i , in line with the technical specification of the device, i.e. 600, 300, 200, 100, 60, 30, 20, 10, 6, 3, 2, 1 rpm. The results of the measurements are enumerated in Table 5. The rheological parameters listed are the average of five measurements made for each rotational speed. Taking into account the coaxial system of cylinders (B1-R1) and the type of the spring (F1), and based on the equations:

$$\dot{\gamma}_i = 1.7034 \cdot n_i \quad (1)$$

$$\tau_i = 0.511 \cdot \Phi_i \quad (2)$$

the relation between the shear rate and shear stresses were determined for each saline slurry (Stryczek 1999). The results of calculations are listed in Table 6.

Based on the results of the measurements and calculations the apparent viscosity of the analysed slurries in the function of shear rate was plotted (Fig. 1).

TABLE 5

Recorded torsions of the spring during measurement of rheological properties of saline slurries with the Chan viscometer

TABLICA 5

Odczyty kąta skręcania sprężyny wykonane podczas pomiaru właściwości reologicznych solankowych zaczynów uzyskane za pomocą lepkościomierza Chan

No	Fly ash content [%]	Torsion of spring [°]	Rotational speed [rpm]											
			600	300	200	100	60	30	20	10	6	3	2	1
1	100	Torsion of spring [°]	105	60	40	21	12	7	5	4	3	2	2	1
2	90		118	63	43	22	13	7	6	4	3	3	2	1
3	80		134	69	47	25	16	9	7	5	4	3	2	1
4	70		138	73	50	27	19	10	8	5	4	4	3	3
5	50		182	97	66	37	24	15	12	9	7	5	5	4
6	30		235	122	81	44	29	18	13	9	7	6	5	4
7	10		267	139	91	53	36	22	17	12	10	8	7	6
8	0		272	144	100	64	48	33	28	22	19	15	12	9

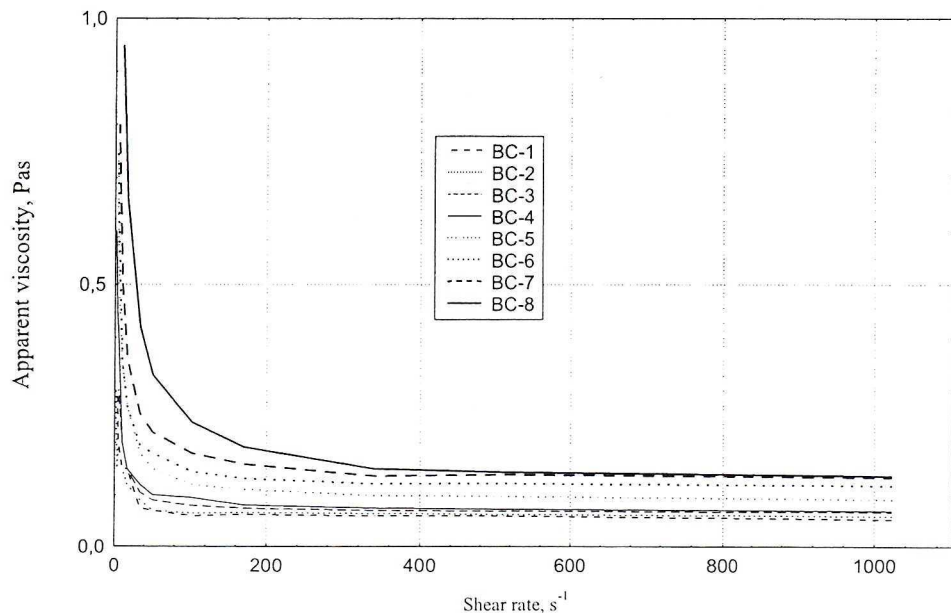


Fig. 1. Dependence of apparent viscosity of the analysed liquid on shear rate

Rys. 1. Zależność lepkości pozornej badanych cieczy od szybkości ścinania

TABLE 6

Dependence of shear stresses on shear rate for the tested saline slurries

TABLICA 6

Zależność naprężen stycznych τ od szybkości ścinania $\dot{\gamma}$ dla analizowanych zaczyńów solankowych

No	Fly ash content [%]		Shear rate $\dot{\gamma}$ [s^{-1}]											
			1022.0	511.2	340.8	170.4	102.2	51.12	34.08	17.04	10.22	5.11	3.41	1.70
1	100	Shear stress. τ [Pa]	53.655	30.66	20.44	10.731	6.132	3.577	2.555	2.044	1.533	1.022	1.022	0.511
2	90		60.298	32.193	21.973	6.643	6.643	3.577	3.066	2.044	1.533	1.533	1.022	0.511
3	80		68.474	35.259	24.017	8.176	8.176	4.599	3.577	2.555	2.044	1.533	1.022	0.511
4	70		70.518	37.303	25.55	6.132	9.709	5.11	4.088	2.555	2.044	2.044	1.533	1.533
5	50		93.002	49.567	33.726	12.264	12.264	7.665	6.132	4.599	3.577	2.555	2.555	2.044
6	30		120.085	62.342	41.391	14.819	14.819	9.198	6.643	4.599	3.577	3.066	2.555	2.044
7	10		136.437	71.029	46.501	18.396	18.396	11.242	8.687	9.709	5.11	4.088	3.577	3.066
8	0		138.992	73.584	51.1	24.528	24.528	16.863	14.308	11.242	9.709	7.665	6.132	4.599

4. Selection of a rheological model and determination of its rheological parameters

To make an optimum choice of the rheological model of the saline sealing slurry based on a specific recipe, the most frequently used models of technological liquids were analysed (Wiśniowski 2000).

TABLE 7

Rheological models of drilling fluids

TABLICA 7

Modele reologiczne cieczy wiertniczych

Model	Rheological function
Newtonian	$\tau = \eta \left(-\frac{dv}{dr} \right)$
Bingham's	$\tau = \tau_y + \eta_p \left(-\frac{dv}{dr} \right)$
Ostwald de Waele's	$\tau = k \left(-\frac{dv}{dr} \right)^n$
Casson's	$\tau = \sqrt{\tau_{yc}} + \sqrt{\eta_{pc}} \sqrt{-\frac{dv}{dr}}$
Herschel Bulkley's	$\tau = \tau_yHB + k_{HB} \left(-\frac{dv}{dr} \right)^n$

The rheological parameters of individual models were calculated according to regression analysis methods. Using the least square method and employing the relations introduced in (Wiśniowski 2001) the following parameters could be defined:

- for the Newtonian model:
 - coefficient of dynamic viscosity

$$\eta = \frac{\sum_{i=1}^{12} \dot{\gamma}_i \tau_i}{\sum_{i=1}^{12} (\dot{\gamma}_i)^2} \quad (3)$$

- for Bingham's model:
 - plastic viscosity

$$\eta_p = \frac{12 \sum_{i=1}^{12} \dot{\gamma} \tau_i - \sum_{i=1}^{12} \dot{\gamma}_i \sum_{i=1}^{12} \tau_i}{12 \sum_{i=1}^{12} \dot{\gamma}_i^2 \left(\sum_{i=1}^{12} \dot{\gamma}_i \right)^2} \quad (4)$$

- flow-behaviour index

$$\tau_y = \frac{\sum_{i=1}^{12} \tau_i - a \sum_{i=1}^{12} \dot{\gamma}_i}{12} \quad (5)$$

- for Ostwald de Waele's model:
 - flow behaviour index

$$n = \frac{12 \sum_{i=1}^{12} (\ln(\dot{\gamma}_i) \ln(\tau_i)) - \sum_{i=1}^{12} \ln(\dot{\gamma}_i) \sum_{i=1}^{12} \ln(\tau_i)}{12 \sum_{i=1}^{12} (\ln(\dot{\gamma}_i))^2 - \left(\sum_{i=1}^{12} \ln(\dot{\gamma}_i) \right)^2} \quad (6)$$

- consistency index

$$k = e^{\left(\frac{\sum_{i=1}^{12} \ln(\tau_i) - n \sum_{i=1}^{12} \ln(\dot{\gamma}_i)}{12} \right)} \quad (7)$$

- for Casson's model:
 - Casson's plastic viscosity

$$\eta_{pc} = \left(\frac{12 \sum_{i=1}^{12} (\sqrt{\dot{\gamma}_i} \sqrt{\tau_i}) - \sum_{i=1}^{12} \sqrt{\dot{\gamma}_i} \sum_{i=1}^{12} \sqrt{\tau_i}}{12 \sum_{i=1}^{12} \dot{\gamma}_i - \left(\sum_{i=1}^{12} \sqrt{\dot{\gamma}_i} \right)^2} \right)^2 \quad (8)$$

- Casson's yield point

$$\tau_{yc} = \left(\frac{12 \sum_{i=1}^{12} \sqrt{\tau_i} - \eta_p \sum_{i=1}^{12} \sqrt{\dot{\gamma}_i}}{12} \right)^2 \quad (9)$$

- for Herschel Bulkley's model:

Herschel Bulkley's flow-bahaviour index n , after solving the equation:

$$12 \sum_{i=1}^{12} (\tau_i \dot{\gamma}_i^n \ln \dot{\gamma}_i) - \sum_{i=1}^{12} \tau_i \sum_{i=1}^{12} (\dot{\gamma}_i^n \ln \dot{\gamma}_i) + \frac{12 \sum_{i=1}^{12} \tau_i \dot{\gamma}_i^n - \sum_{i=1}^{12} \tau_i \sum_{i=1}^{12} \dot{\gamma}_i^n}{12 \sum_{i=1}^{12} \dot{\gamma}_i^{2n} - \sum_{i=1}^{12} \dot{\gamma}_i^n \sum_{i=1}^{12} \dot{\gamma}_i^n} \cdot \sum_{i=1}^{12} \dot{\gamma}_i^n \sum_{i=1}^{12} (\dot{\gamma}_i^n \ln \dot{\gamma}_i) - 12 \sum_{i=1}^{12} (\dot{\gamma}_i^n \ln \dot{\gamma}_i) = 0 \quad (10)$$

The algorithm of numerical solution of equation (10) was presented in (Wiśniowski 2001).

- Herschel Bulkley's consistency index:

$$k_{HB} = \frac{12 \sum_{i=1}^{12} \tau_i \dot{\gamma}_i^n - \sum_{i=1}^{12} \tau_i \sum_{i=1}^{12} \dot{\gamma}_i^n}{12 \sum_{i=1}^{12} \dot{\gamma}_i^{2n} - \sum_{i=1}^{12} \dot{\gamma}_i^n \sum_{i=1}^{12} \dot{\gamma}_i^n} \quad (11)$$

- Herschel Bulkley's yield point:

$$\tau_{yHB} = \frac{\sum_{i=1}^{12} \tau_i - k \sum_{i=1}^{12} \dot{\gamma}_i^n}{12} \quad (12)$$

The optimum rheological model was selected after special statistical tests. After defining rheological parameters for each analysed model, standard deviation of the obtained regression coefficients was calculated, and then their significance level established (t-Student test) (Godziszewski et al. 1982). Next the sum of the least squares U and standard error ε were determined.

The considerable discrepancy between the results (shear stress) τ calculated from the model and the actual measured values τ was established through the correlation coefficient R (Volk 1999). The significance of the calculated correlation coefficient and the adequacy of the mathematical model were evaluated through the application of the Fischer-Snedecor test (Godziszewski et al. 1982)

From among the analysed models in which the correlation coefficient has significance, the model with the highest correlation coefficient was taken as optimum.

Due to the large number of calculations and the need to use numerical methods and statistical tests, a special numerical programme Flow_Fluid_Coef (elaborated in the Department of Drilling and Geo-engineering, UMM) was employed. The results of the calculations and analyses are shown in Table 8.

It can be stated from the results of calculations that all the analysed rheological models have a very good correlation ($R > 0.9$) with the results of the sealing slurries

TABLE 8

Results of calculated rheological parameters for individual sealing slurry models

TABLICA 8

Wyniki obliczeń parametrów reologicznych poszczególnych modeli zaczynów uszczelniających

Fly ash content [%]	Rheological model	Equation	Correlation coefficient	Fischer-Snedecor coefficient
1	2	3	4	5
100	Newtonian	$\tau = 0.0548 \cdot \dot{\gamma}$	0.9959	1 202
	Bingham's	$\tau = 1.13 + 0.0530 \cdot \dot{\gamma}$	0.9980	2 486
	Ostwald de Waele's	$\tau = 0.31 \cdot \dot{\gamma}^{0.7053}$	0.9632	402
	Casson's	$\sqrt{\tau} = 0.469 + 0.21 \cdot \sqrt{\dot{\gamma}}$	0.9989	3 459
	Herschel Bulkley's	$\tau = -3.84 + 0.99 \cdot \dot{\gamma}^{0.5728}$	0.9819	268
90	Newtonian	$\tau = 0.0604 \cdot \dot{\gamma}$	0.9983	2 897
	Bingham's	$\tau = 1.01 + 0.0588 \cdot \dot{\gamma}$	0.99949	9 853
	Ostwald de Waele's	$\tau = 0.33 \cdot \dot{\gamma}^{0.7031}$	0.9537	101
	Casson's	$\sqrt{\tau} = 0.480 + 0.22 \cdot \sqrt{\dot{\gamma}}$	0.99948	9 619
	Herschel Bulkley's	$\tau = -4.10 + 0.99 \cdot \dot{\gamma}^{0.5873}$	0.9794	235
80	Newtonian	$\tau = 0.068 \cdot \dot{\gamma}$	0.9985	3 281
	Bingham's	$\tau = 1.21 + 0.0661 \cdot \dot{\gamma}$	0.9999	34 974
	Ostwald de Waele's	$\tau = 0.36 \cdot \dot{\gamma}^{0.7158}$	0.9654	137
	Casson's	$\sqrt{\tau} = 0.538 + 0.24 \cdot \sqrt{\dot{\gamma}}$	0.9996	11 934
	Herschel Bulkley's	$\tau = -4.13 + 0.99 \cdot \dot{\gamma}^{0.5478}$	0.9861	244
70	Newtonian	$\tau = 0.0707 \cdot \dot{\gamma}$	0.9968	1 539
	Bingham's	$\tau = 1.8 + 0.0680 \cdot \dot{\gamma}$	0.9996	14 049
	Ostwald de Waele's	$\tau = 0.63 \cdot \dot{\gamma}^{0.6207}$	0.9310	65
	Casson's	$\sqrt{\tau} = 0.73 + 0.23 \cdot \sqrt{\dot{\gamma}}$	0.9995	9 716
	Herschel Bulkley's	$\tau = -3.64 + 0.99 \cdot \dot{\gamma}^{0.6083}$	0.9828	282

1	2	3	4	5
50	Newtonian	$\tau = 0.0935 \cdot \dot{\gamma}$	0.9954	1 084
	Bingham's	$\tau = 2.87 + 0.0891 \cdot \dot{\gamma}$	0.9997	15 164
	Ostwald de Waele's	$\tau = + 0.55 \cdot \dot{\gamma}^{0.6394}$	0.9333	68
	Casson's	$\sqrt{\tau} = 0.98 + 0.27 \cdot \sqrt{\dot{\gamma}}$	0.9993	6 942
	Herschel Bulkley's	$\tau = -3.19 + 0.99 \cdot \dot{\gamma}^{0.6477}$	0.9869	375
30	Newtonian	$\tau = 0.1193 \cdot \dot{\gamma}$	0.9978	2 292
	Bingham's	$\tau = 2.60 + 0.1153 \cdot \dot{\gamma}$	0.9999	52 683
	Ostwald de Waele's	$\tau = 0.97 \cdot \dot{\gamma}^{0.6360}$	0.9329	67
	Casson's	$\sqrt{\tau} = 0.89 + 0.31 \cdot \sqrt{\dot{\gamma}}$	0.9990	4 760
	Herschel Bulkley's	$\tau = -3.99 + 0.99 \cdot \dot{\gamma}^{0.6851}$	0.9879	407
10	Newtonian	$\tau = 0.1359 \cdot \dot{\gamma}$	0.9961	1 267
	Bingham's	$\tau = 3.89 + 0.1299 \cdot \dot{\gamma}$	0.9998	20 545
	Ostwald de Waele's	$\tau = 1.46 \cdot \dot{\gamma}^{0.5922}$	0.9253	60
	Casson's	$\sqrt{\tau} = 1.17 + 0.32 \cdot \sqrt{\dot{\gamma}}$	0.9984	3 134
	Herschel Bulkley's	$\tau = -2.97 + 0.99 \cdot \dot{\gamma}^{0.7024}$	0.9894	463
0	Newtonian	$\tau = 0.1412 \cdot \dot{\gamma}$	0.9809	255
	Bingham's	$\tau = 8.38 + 0.1282 \cdot \dot{\gamma}$	0.9986	3 522
	Ostwald de Waele's	$\tau = 3.00 \cdot \dot{\gamma}^{0.4961}$	0.9325	67
	Casson's	$\sqrt{\tau} = 1.96 + 0.94 \cdot \sqrt{\dot{\gamma}}$	0.9977	2 152
	Herschel Bulkley's	$\tau = 1.46 + 0.99 \cdot \dot{\gamma}^{0.7008}$	0.9913	567

analysed. The degree of correlation of a given rheological model does not depend on the ash content of the mixture. However, as far as the physical sense of the obtained parameters of rheological models is concerned, it can be stated that the Herschel-Bulkley's model should *not* be used when describing sealing slurring with fly ash content. The negative value of yield point in this model cannot be interpreted physically.

The solution of brine and fly ash without cement content (BC-1) can be best described with Casson's model. In the remaining cases it is Bingham's model, the function of which depends on the ash content in the mixture (Table 8) that provides the most lucid description.

The analysis of the results listed in Table 8 shows that the rheological parameters grow with the increasing cement content. This phenomenon can be explained by the fact that the cement composition (influencing the hydration process) decides about the rheological properties of fresh slurries.

During hydration processes a significant quantity of gypsum goes into solution, saturating the liquid phase with Ca^{2+} and SO_4^{2-} ions and alkalies making up the cement. During the first stage of hydration, certain quantities of ettringite are formed. If making a compact film on the cement grains, ettringite does not significantly affect the rheological structure of the slurry. At this stage of induction the alite reactions with water do not influence the structure of the slurry, provided it was so mixed as to sever the hydrates from the surface of the cement grains. After a long induction, the rheological properties significantly deteriorate due to the crystallisation of $\text{Ca}(\text{OH})_2$ and accelerated hydration of alite. The intensity of these changes is the function of time and the chemical-mineral composition of the cement.

In cements with low calcium tri-aluminates (C_3A) the liquid phase is saturated with calcium sulphate which behaves as a strong flocculent. It reduces dissolved calcium aluminates and simultaneously accelerates silica hydration.

At a high C_3A content in the cement the ettringite crystallises and the sulphate ion content falls. These processes are caused by the existing series of water reactivities of mineral components making up the clinker cement: C_3A , C_3S , C_4AF , $\beta\text{C}_2\text{S}$ (Stryczek 1998).

To sum up, the influence of the initial chemical reactions on hydration processes and physical properties, and so the rheological parameters of fresh slurries, is progressively greater with an increase of:

- C_3A content in cement,
- specific surface (grain size) of cement,
- cement concentration in the slurry (water-to-cement ratio).

5. Determining of frictional pressure loss of saline sealing slurries described with Bingham's model

When determining the parameters of the rheological model it is possible to define the frictional pressure loss of flow of the saline sealing slurry in a circulation system.

To calculate the pressure losses in the injection pipe (inner diameter d_w and length l) due to the flow of a volume Q of a saline sealing slurry, described by Bingham's model, it is necessary to first determine the flow rate and the range of flow:

- the fluid velocity of the slurry from the equation:

$$\nu = \frac{4Q}{\pi d_w^2} \quad (13)$$

- character of flow, and establishing the Hedstrom number:

$$He = \frac{\rho \cdot d_w^2 \cdot \tau_y}{\eta_p^2} \quad (14)$$

and then the critical Reynolds number from the nomogram in Fig. 2

The flow can be treated as laminar if $Re < 2100$.

Depending on the flow range the losses of hydraulic pressure of saline sealing slurry described with Bingham's model should be calculated:

- for turbulent flow from the equations:
 - for pipes with joint of JP or WP type

$$p = \frac{0.094 \eta_p^{0.21} \rho^{0.79} \nu^{1.79} l}{d_w^{1.21}} \quad (15a)$$

- for pipes with joints of SP type

$$p = \frac{0.072 \eta_p^{0.17} \rho^{0.83} \nu^{1.83} l}{d_w^{1.17}} \quad (15b)$$

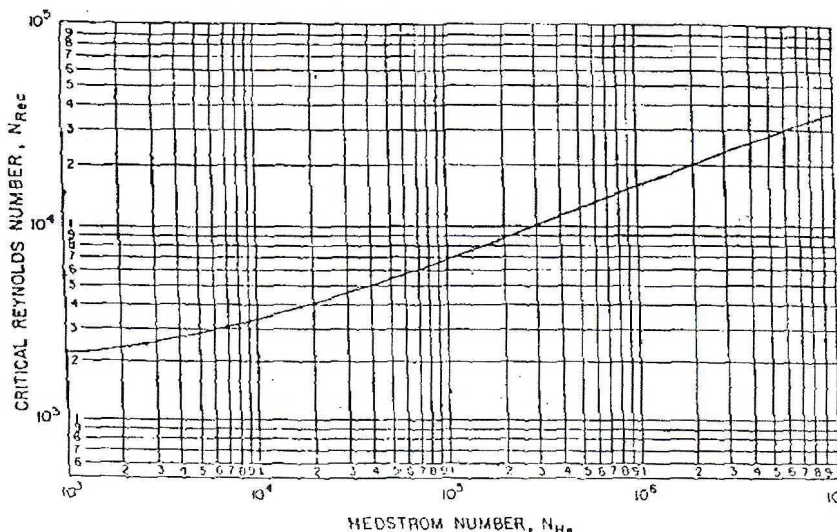


Fig. 2 Relation of critical Reynolds number for Bingham's liquid and Hedstrom's number (Bourgoyne et al. 1986)

Rys. 2. Zależność wartości krytycznej liczby Reynoldsa dla cieczy binghamowskiej od liczby Hedstroma (Bourgoyne et al. 1986)

- for laminar flow, after unit pressure losses were established and equation 9 solved:

$$Q = \frac{\pi d_w^4}{128 \eta_p} \left(\frac{dp}{dl} - \frac{16}{3} \frac{\tau_y}{d_w} + \frac{1}{3} \frac{dp}{dl} \left(\frac{4\tau_y}{d_w \cdot \frac{dp}{dl}} \right)^4 \right) \quad (16)$$

The equation (16) is a complex equation with one variable, i.e. unit flow frictional pressure loss dp/dl . Solving it requires one of the numerical methods (shear method, secant method, combined methods). Here a function is written in the following form

$$g(x) = \frac{\pi d_w^4}{128 \eta_p} \left(x - \frac{16}{3} \frac{\tau_y}{d_w} + \frac{1}{3} x \left(\frac{4\tau_y}{d_w \cdot x} \right)^4 \right) - Q \quad (17)$$

and then its zero point is determined.

To do this, an interval $[a, b]$ is established with the searched element. Bearing in mind the physical sense of the searched parameter we assume $x \in [0, 10000]$.

The zero point of $g(x)$ in $[a, b]$ is determined through the method of bisection (Fig. 3)

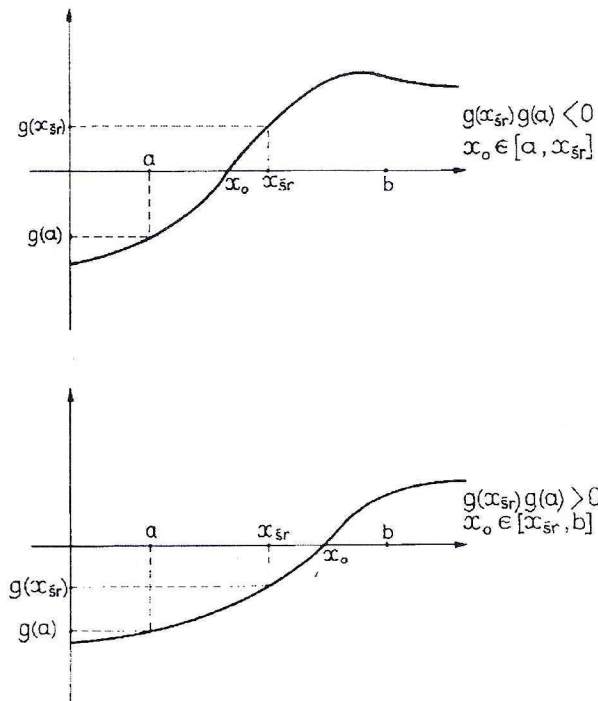


Fig. 3 Determining of element of function $g(x)$ through the method of bisection

Rys. 3. Wyznaczenie pierwiastka funkcji $g(x)$ metodą połówienia przedziału

Initially the interval is divided into two and the average value calculated $x_{sr} = (a + b)/2$. Next $g(x_{sr})$ is calculated and compared with $g(a)$. If the sign of the function changes, then the function $g(x)$ stays within $[a, x_{sr}]$, otherwise in $[x_{sr}, b]$.

The calculations are made when the width of the interval is smaller or equal to the predefined ε . Then the elements of the function are calculated from the equation $x_{sr} = (a - b)/2$.

A numerical programme was elaborated in the Department of Drilling and Geo-engineering, UMM thanks to which equation (16) could be solved using the method of bisection. The assumed limits of the searched solution ($x_{sr} = dp/dl$) were assumed as follows: $a = 1$, $b = 10^4$, accuracy $\varepsilon = 0.00001$. Having all unit frictional pressure loss of a laminar flow of a saline slurry determined, the sum of the pressure losses in the pipe (d_w inner diameter and length l) should be calculated from the equation:

$$p = x_{sr} \cdot l \quad (18)$$

The algorithm of solution of equation (17) with the method of bisection is presented in Fig. 4.

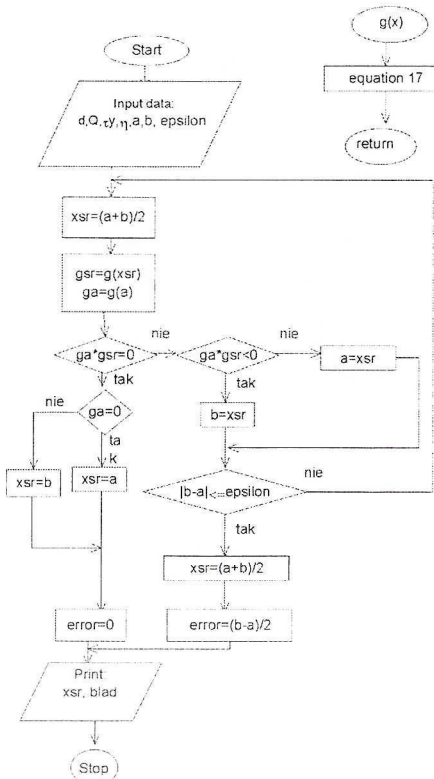


Fig. 4. Block diagram of solving function $g(x)$ for $[a, b]$ using method of bisection

Rys. 4. Schemat blokowy obliczania pierwiastka funkcji $g(x)$ znajdującego się w przedziale $[a, b]$ z wykorzystaniem metody połówienia przedziału

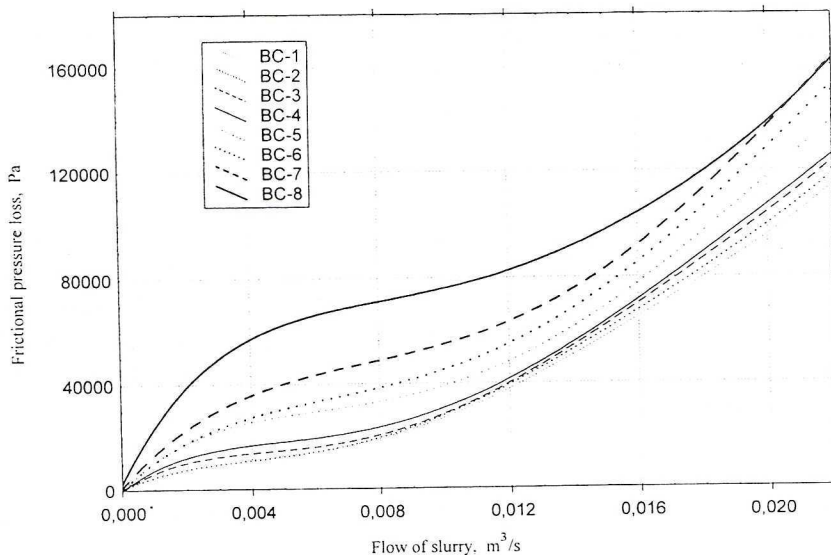


Fig. 5. Frictional pressure-loss of flow for different slurry recipes in the function of flow rate: inner diameter of injection pipes: $d_w = 0.1086 \text{ m}$, length of the pipes: $l = 100 \text{ m}$

Rys. 5. Wielkość oporów przepływu różnych receptur solankowych zaczynów uszczelniających w funkcji strumienia przepływu: średnica wewnętrzna rur tłoczących: $d_w = 0,1086 \text{ m}$, długość rur tłoczących: $l = 100 \text{ m}$

Based on the methods outlined above, the frictional pressure losses were simulated for the analysed recipes and the Bingham model. The following assumptions were made: liquid density as in the Table 4, inner diameter of injection pipes: $d_w = 0.1086 \text{ m}$ (NC50 4 1/2 IF), length of the pipes: $l = 100 \text{ m}$, injection rate $Q \in (0.0 - 0.022 \text{ m}^3/\text{s})$.

The changes of the injected volume result from the characteristics of the cementing device CA-320 with which the injection of the slurry is to be made. The results of the simulation have been listed in Fig. 5.

6. Summary and conclusions

The recipes for ash-cement saline sealing slurries used for filling the voids in the rock mass should meet certain requirements: environmental compatibility, injectability, strength and long life of the hardened cement, and economical-environmental feasibility.

By assuming a given rheological model of the saline sealing slurry with fly ash content one should use algorithms and computer programmes.

It can be stated on the basis of the tests conducted and the analyses of saline sealing slurries with fly ash content that all the analysed models have a good correlation with the results of the analysed sealing slurries, and the degree of correlation of a given rheological model does not depend on the fly ash content of the mixture.

The solution of the brine and fly ashes without cement admixtures (BC-1) is best described by Casson's model. In the remaining cases it is Bingham's model which best approximates the to measurement data, and which takes account of the fly-ash content in the mixture.

By increasing the ash content in the analysed liquid the frictional pressure loss of flow of the saline sealing slurries based on fly ashes can be considerably lowered.

Paper prepared within statute research programme No 11.190.01 at the Faculty of Drilling Oil and Gas, University of Mining and Metallurgy, Cracow

REFERENCES

- Bourgoyn A.T., Milheim K.K., Chenevert M.E., Young F.S., 1986. Applied Drilling Engineering, SPE, Textbook.
- Godziszewski J., Mania R., Pamuch R., 1982. Zasady planowania doświadczeń i opracowywania wyników pomiaru. Skrypt nr 871, AGH, Kraków.
- Orzeczenie o jakości cementu. CEM I 32,5 R. Górażdże Trade Spółka z o.o., Chorula 2000.
- Praca zbiorowa: Badania fizykochemiczne popiołów z Elektrocieplowni Kraków S.A. Instytut Gospodarki Przestrzennej i Komunalnej Oddział w Krakowie. Zleceniodawca: Elektrocieplownia Kraków S.A., Kraków 2000.
- Stryczek S., Gonc A., 2001. Solankowe zaczyny popiołowo-cementowe. Zeszyty naukowe AGH. Wiertnictwo, Nafta, Gaz z. 18, Kraków.
- Stryczek S., 1998. Wpływ stopnia rozdrobnienia spoiw hydraulycznych na właściwości reologiczne zaczynów uszczelniających. Zeszyty naukowe AGH, Górnictwo z. 3, Kraków.
- Stryczek S., 1999. Wyznaczanie parametrów reologicznych płuczek wiertniczych, Nowoczesne Techniki i Technologie Bezwykopowe z. 2, Kraków.
- Volk W., 1973. Statystyka stosowana dla inżynierów. Wydawnictwa Naukowo-Techniczne, Warszawa .
- Wiśniowski R., 2000. Zastosowanie modelu Herschel-Bulkleya w hydraulice płuczek wiertniczych. Nowoczesne Techniki i Technologie Bezwykopowe z. 2, Kraków.
- Wiśniowski R., 2001. Metodyka określania modelu reologicznego cieczy wiertniczej. Zeszyty naukowe AGH. Wiertnictwo, Nafta, Gaz z 18, Kraków.

REVIEW BY: PROF. DR HAB. INŻ. JAKUB SIEMEK, KRAKÓW

Received: 19 March 2001